

promoting access to White Rose research papers



Universities of Leeds, Sheffield and York
<http://eprints.whiterose.ac.uk/>

This is a final published version of a paper accepted for publication in
International Journal of Fuels and Lubricants.

White Rose Research Online URL for this paper:

<http://eprints.whiterose.ac.uk/42889/>

Paper

Li, H, Andrews, GE, Savvidis, D, Daham, BK, Ropkins, K, Bell, MC and Tate, JE
(2009) *Impact of Driving Cycles on Greenhouse Gas (GHG) Emissions, Global
Warming Potential (GWP) and Fuel Economy for SI Car Real World Driving.*
International Journal of Fuels and Lubricants,1 (1). 1320 -1333.

Copyright (c) 2008 SAE International. Further use or distribution of this paper is
not permitted without permission from SAE.

<http://saefuel.saejournals.org/content/1/1/1320.abstract>

Impact of Driving Cycles on Greenhouse Gas (GHG) Emissions, Global Warming Potential (GWP) and Fuel Economy for SI Car Real World Urban Driving

Hu Li, Gordon E Andrews, Dimitrios Savvidis and Basil Daham
Energy and Resources Research Institute

Karl Ropkins, Margaret Bell and James Tate
The University of Leeds

Copyright © 2008 SAE International

ABSTRACT

The transport sector is one of the major contributors to greenhouse gas emissions. This study investigated three greenhouse gases emitted from road transport: CO₂, N₂O and CH₄ emissions as a function of engine warm up and driving cycles. Five different urban driving cycles were developed and used including free flow driving and congested driving. An in-vehicle FTIR (Fourier Transform Infrared) emission measurement system was installed on a EURO2 emission compliant SI (Spark Ignition) car for emissions measurement at a rate of 0.5 HZ under real world urban driving conditions. This emission measurement system was calibrated on a standard CVS (Constant Volume Sampling) measurement system and showed excellent agreement on CO₂ measurement with CVS results. The N₂O and CH₄ measurement was calibrated using calibration gas in lab. A MAX710 real time in-vehicle fuel consumption measurement system was installed in the test vehicle and real time fuel consumption was then obtained. The temperatures across the TWC (Three Way Catalyst) and engine out exhaust gas lambda were measured. The GHG (greenhouse gas) mass emissions and consequent GWP (Global Warming Potential) for different urban driving conditions were analyzed and presented. The results provided a better understanding of traffic related greenhouse gas emission profile in urban area and will contribute to the control of climate change.

INTRODUCTION

As a part of global effort to control the climate change, the UK government has agreed to reduce emissions of a basket of six greenhouse gases (CO₂, CH₄, N₂O,

HFCs, PFCs and SF₆) by 12.5% from base year by 2008~2012. The base year is 1990 for CO₂, CH₄ and N₂O and 1995 for HFCs, PFCs and SF₆.

The Greenhouse gases produced by transport sectors include CO₂, methane and nitrous oxide. CO₂ is a dominant GHG and has been extensively investigated. Currently the CO₂ emissions from transport sector accounted for around 28% of total CO₂ emissions in the UK. The methane emissions mainly come from landfill sites and agriculture sector, which were 38% and 36% in the UK in year 2004. The transport sector only contributed a small fraction of total methane emissions. Transport sector is an important contributor to nitrous oxide emissions.

This project is part of a major study of real world emissions and the traffic control and road system impacts on real world vehicle emissions. In the present work the important influence of driving cycles on urban passenger SI car GHG emissions is investigated. Five different real world urban driving cycles were developed to simulate free flow, junctions, congested traffic and medium speed cruising etc.

A Euro 2 vehicle was used as they are one of the major proportions of the UK vehicle fleet and hence major contributors to air pollution in cities. The ongoing work is investigating Euro 3 and 4 vehicles. It takes about 16 years for 90% of vehicles sold in any one year to be no longer in use [1] and this period becomes longer for modern vehicles. Thus the work on EURO 2 vehicles has significance in terms of their current use in city driving and hence their impact on air quality. It will be at least 2010 before 90% of EURO 2 vehicles are not a significant proportion of city traffic [2]. This work on EURO 2 vehicles will also be the basis for future work on the influence of ambient

temperature and vehicles that meet subsequent lower emissions standards.

The significance of this real world test program lies in that this test represented the whole vehicle response to cold start, including gearbox and cold tyre effects that can not be achieved by dynamometer tests. This research investigated engine thermal performance, fuel consumption, GHG emission behaviors and GWP under different urban driving conditions, which can be used for a better understanding of the vehicle response in the real world driving conditions and provide valuable information to modelers for better prediction of emissions and air qualities in cities.

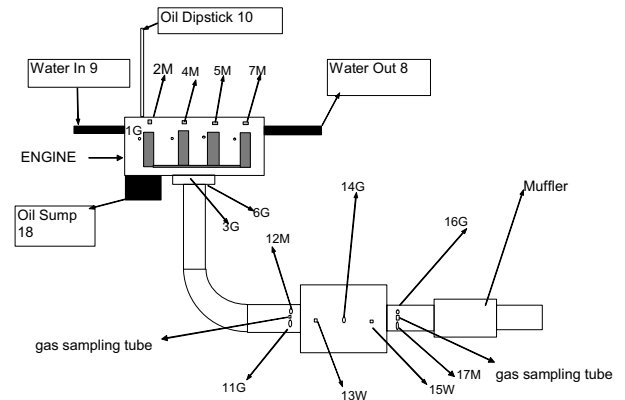
This work is part of a major research project RETEMM (REal-world Traffic Emissions Measurement and Modeling), which is part of the LANTERN research programme (Leeds health Air quality, Noise, Traffic, Emissions Research Network). One of the purposes of the RETEMM project is to investigate the emissions characteristics under real world driving conditions, including the influence of ambient temperatures, driving cycles, traffic conditions and vehicle technologies etc [3-8].

EXPERIMENTAL

TEST CAR AND THERMAL MEASUREMENT

A Ford Mondeo manual transmission petrol car was used, which was fitted with a port fuel injected 2.0 litre 16V Zetec spark ignition engine with 4 cylinders and 16 valves. The odometer reading on the car was 85,000 miles. The vehicle was equipped with a Three Way Catalyst (TWC). The curb weight of the car is 1360 kg. The car was instrumented with 19 thermocouples, which measured the air inlet, engine coolant and lubricating oil temperatures. In addition the exhaust skin (metal), exhaust gas, catalyst and ambient temperatures were also measured. All temperatures were measured using grounded junction mineral insulated Type K thermocouples.

Table 1 identifies the thermocouples by number, location and function. These references are used in the schematic view of the thermocouple locations on the test car (figure 1) and the later graphical presentation of the warm-up temperature results in real-world urban driving. Figure 2 presents the outline of the measurement system and data logging system that was used. A differential GPS system was used to measure the vehicle's travel speed and distance, and this was connected to an analog Daqview data logger along with all 19 thermocouples, fuel consumption and lambda data. The data logger was then connected to a second laptop PC. The thermal measurements were logged at 1Hz and the FTIR emission measurements at 0.5 Hz.



Note:
G is thermocouples for gas.
M and W are thermocouples for metal and catalyst wall.

Figure 1: Schematic view of thermocouple locations

Table 1: Thermocouple locations and functions

The number of thermocouple	The measuring target
1G	Engine out gas temperature from cylinder 1
3G, 6G	Top and bottom side of manifold gas temperature
2M, 4M, 5M 7M	Metal temperature at four different locations on the manifold to monitor overall thermal profile of manifold
8, 9	Coolant water out and in temperature from the engine
11G,14G,16G	Gas temperature at the upstream (11), between the two catalyst bricks (14) and downstream of the TWC (16).
12M,17M	Upstream and downstream of TWC face temperature
13W, 15W	TWC brick temperature
10, 18	Engine oil temperature in dipstick top layer (10) and sump bottom (18)
19 (not shown in graph)	Ambient temperature

ON BOARD EMISSION MEASUREMENT

A portable Fourier Transform Infrared (FTIR) spectrometer was used to measure on-road real world emissions. The model used was the Temet Gaset CR 2000 which was capable of measuring concentrations as low as 0.5~3 ppm, depending on the applications. It has an accuracy of 2% within the calibrated measurement range, which was 30% for CO₂, 1000 ppm for CH₄ and 500 ppm for N₂O respectively. This FTIR measurement was calibrated against standard CVS measurement by authors using a chassis dynamometer facility and various driving cycles [9]. It was found that the FTIR measurement had excellent agreement with the CVS measurement.

The Temet instrument comprised a FTIR analyser, a portable sample handling unit (filtering and controlling

sample flow), heated sample lines and a laptop. The system weighed approximately 30 kg. The entire on-board measurement instrumentation including the FTIR system, the fuel consumption measurement system, two batteries and a DC-AC converter weighed approximately 150 kg.

The software of the FTIR system has the additional capability of accepting analog inputs, which can be logged together with the emissions spectra and analysis data. One of these analog inputs was employed to log throttle position. Two laptops were used for data logging: One for FTIR that logs emission spectra and throttle position; the other one for thermal and driving parameters that logs GPS road speed, fuel mass flow, throttle position, air/fuel ratio and ambient temperature.

The two laptops were time aligned using the throttle position measurement that was logged by both. Figure 2 shows the schematic view of the FTIR emissions measurement system, fuel consumption measurement system and data logging system.

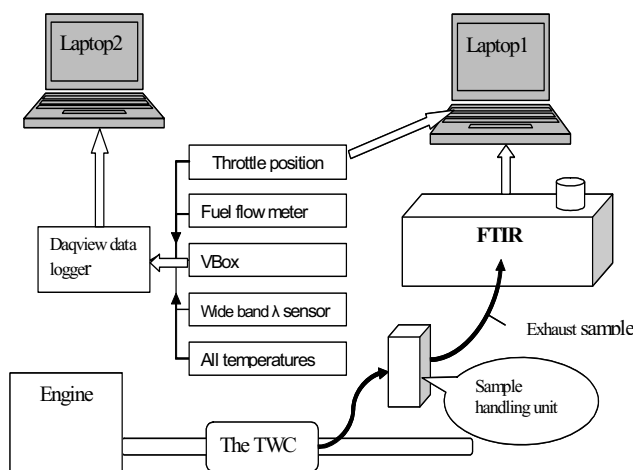


Figure 2: Schematic view of sampling and data logging system

FUEL CONSUMPTION MEASUREMENT

A MAX710 fuel flow measurement system was used to measure real world fuel consumptions. This measured the fuel mass flow rate using a level controlled recirculation tank, transfer pump and a high-resolution flow meter. The pump maintained a constant pressure to the recirculation tank that fed fuel to the engine. This recirculation tank collected return fuel from the engine and recirculated this fuel back to the engine instead of returning it to the fuel tank. This recirculation loop allowed the use of a single meter to measure make-up fuel as it replaced the fuel consumed by the engine. Total fuel consumption was determined to better than 1% accuracy. The rate of fuel consumption was determined at a 1-second resolution. The device had an analog output that was logged onto the second laptop computer.

Commercially available standard ultra low sulfur RON95 petrol fuel was used throughout the tests.

SOURCE OF POWER

The power needed for the on-board measuring system was around 1200 Watts and this would have necessitated drawing up to 100 A at 12V from the car's electrical system. This would have required an upgraded alternator and increased the load on the engine, therefore affecting the emissions characteristics. Another possibility was to use a small dedicated generator but this option is only feasible in large heavy duty vehicles. Therefore, a dedicated power supply, two 12V battery packs and an on-board DC-AC converter, were used to provide 240V AC necessary for instrument operation. The two batteries used weighed a total of 70 kg. They provided approximately 2-3 hours of operation before needing recharging.

SAMPLE CONDITIONING

In order to measure wet concentration, the raw undiluted sample gas extracted from the exhaust system had to be maintained at about 180°C otherwise low boiling point pollutants would drop out due to condensation. Furthermore, the extracted exhaust sample had to be hot filtered so that the sample cell remained free of particulates which would contaminate it and shorten its lifetime. A sample handling unit was acquired to perform these functions. The sample handling unit uses a pump to continuously extract sample from the vehicle's exhaust system at a constant flow rate (2~3 l/min) via a heated line. This is then filtered using a 0.2 µm filter and introduced via another heated line into the sample cell of the FTIR. Both heated lines were maintained to 180°C by the sample handling unit. The sample handling unit consumed the most power since it performed heating and pumping functions. It was installed in the boot of the car along with the FTIR. The gas sample was taken downstream of the catalyst and the heated sample line was passed through a small hole in the car's floorpan. There was no possibility of dilution of the sample by pressure pulsations from the tailpipe.

MASS EMISSION CALCULATION

The FTIR emission measurements were on a volumetric basis. These were converted into a mass basis using the conventional method for the computation of emissions index (EI: g/kg fuel)

$$EI = K * C * (1 + A/F) * 1000 \text{ g/kg fuel} \quad \text{----- (1)}$$

- K is conversion coefficient, which is the ratio of molecular weight of a certain emission component to the molecular weight of the whole sample gas. The molecular weight of the exhaust sample gas is close to that of air and does not vary more than 1% for H/C ratios of about 2 (i.e. gasoline), irrespective of the air/fuel ratio. For this reason, K is here treated as a constant.

- C is concentration of the component. If this is measured in ppm or % then the equation has to be multiplied by 10^{-6} or 10^{-2} respectively.
- A/F is the air/fuel ratio on a mass basis measured by lambda sensor.

The EI was then converted into mass emission rate g/s using fuel consumption measured for the sampling period. Then the distance based emissions can be calculated for any distance traveled.

DRIVING ROUTES AND CYCLES

Five driving cycles were selected for the emission tests. These five driving cycles are: LU-BS (Leeds University-Business School, hereafter referred as BS cycle), LU-Headingley (Leeds University-Headingley, hereafter referred as Headingley cycle), LU-HR-part1 (part 1 of the Leeds University-Headingley Ring road cycle, hereafter referred as HR-part1 cycle) and LU-HPL-A/B (Leeds University-Hyde Park Loop-A/B, hereafter referred as HPL-A/B; A is anticlockwise loop and B is clockwise loop).

The BS driving cycle is previously known as LU-UDTC (Leeds University-Urban Driving Test Cycle) [3]. Figure 3 shows the route of the test cycle. Leeds is a metropolitan district and has a high population density of around $1,300/\text{km}^2$. There is a network of roads with many 90° turns. The car was started from the authors' engine bay dynamometer laboratory, which was close to a public road. The car was parked outside the laboratory and cold soaked for at least five hours prior to testing.

The cold start sampling was started before the ignition on. The vehicle was first driven about 70m to the public road, where it was then driven around the street test circuit shown in figure 3. This had a downhill and uphill portion on the top left part of the circuit in figure 3, the rest of the circuit was flat. There were seven 90° turns in the circuit, 5 of them left hand turns.

At the end of each lap of the 1.45 km test circuit the vehicle was stopped in a car park and then the circuit was repeated. The first cold-start circuit was thus slightly different to the other three circuits. The main road to the right of figure 3 was a very busy major road with one of the highest traffic densities for an urban road in the UK. However, the traffic densities on the test circuit were much lower and the repeatability of each lap was not greatly influenced by differences in traffic loads.

The distance traveled for each lap was 1.45 km, giving a total distance for the four laps of 5.8 km. It involved 18~21 gear changes for each lap, depending on the traffic conditions. The speed limit on these urban streets was 48 km/h (30 mph) and the peak speed never exceeded this, as shown in figure 4. Each section of the route involved acceleration from a 90° corner turn up to a peak speed close to the speed limit

and then a deceleration to the next corner. Six or seven deceleration and acceleration modes were involved in each lap of the route. There were also short periods of idling between the laps due to traffic conditions.

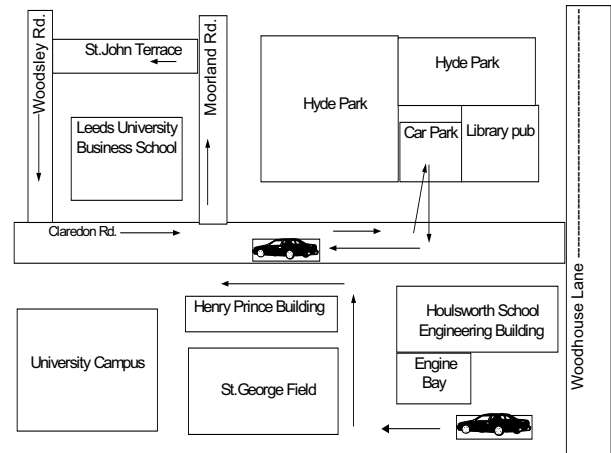


Figure 3: The route of BS driving cycle

The second driving cycle Headingley is one of the typical congested main urban commuter roads in Leeds. The journey started from the University (big star sign in the figure 4) and ended at West Park Roundabout (small star sign in figure 4). The distance traveled was 4.4 km. It passed 5 crossroads with traffic lights, 6 pedestrian lights and 9 give way junctions. The Headingley cycle does not involve any turns and all speed changes are caused by road traffic events.

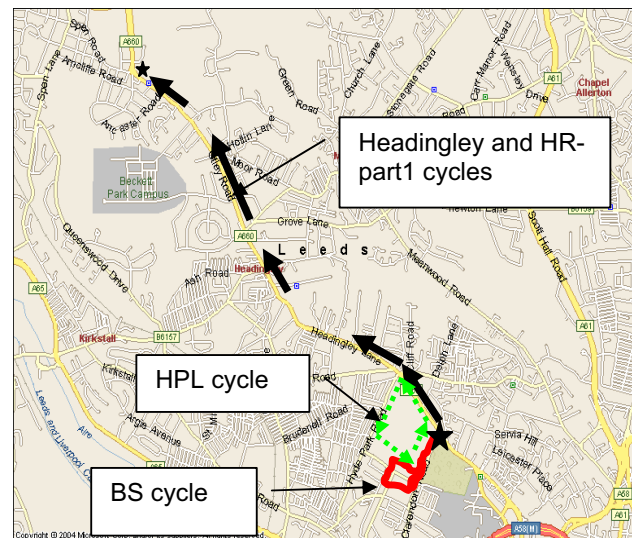


Figure 4: The route of Headingley driving cycle along with BS and HPL cycles.

The third driving cycle HR-part1 is the first part of a driving cycle HR. For the HR cycle, the vehicle was driving passing the west park roundabout (small star sign in figure 4) and continued to travel for approximately 400 m and then turned right into Leeds out ring road, where the national speed limit applies. i.e. the vehicle can drive up to 112 km/h (70mph). In

this study, only the first 1000 seconds of HR cycle was presented and referred as the HR-part1 as this was representing the cold start section of the HR cycle and comparable to other test cycles. The emission profile of whole HR cycle will be presented in a separated paper. The route of the HR-part1 in this study can be referred to figure 4. In fact, the journey used in this paper for HR-part1 driving cycle was a congested journey and the distance traveled was just over 4 km, which was shorter than Headingley cycle. So the Headingley journey and HR-part1 journey in this paper were driving on the same route but represented two different traffic situations: slightly congested Headingley journey and very congested HR-part1 journey.

The fourth and fifth driving cycles Leeds-HPL-A or B were a 1.96 km loop circuit, located in a busy residential area linked with major roads as shown in figure 5. The HPL-A cycle is driving in anticlockwise direction and HPL-B is driving in clockwise direction. Of the cycle, side AB was a dual carriage way on which the vehicle can travel up to ~60 km/h and have less traffic interferences. The other three sides were two-way single carriageways on which the vehicle can travel up to 48 km/h but with more traffic variation and interferences. The sides CD and DA have a set of pedestrian light on each road. Junction A, B and D are traffic light controlled. For HPL-A, the driving at junctions A, B and D will depend on traffic light status to stop or driving through and at junction C there will be not stop. For HPL-B, the driving at junctions will not only controlled by the traffic lights but also subject to oncoming straight traffic and therefore has longer stops.

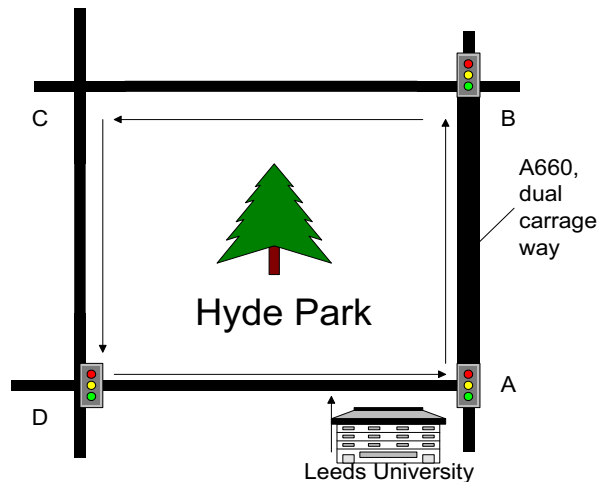


Figure 5: The route of HPL driving cycle

One example journey for each driving cycle was selected in this paper for the analysis of driving parameters and emissions. These examples may not be able to represent all features of the particular cycle but they represented most features of the traffic conditions of the particular cycle. Table 2 shows the summary of the five driving cycles for driving features and traveled distance.

Table 2: Summary of driving cycles

Name of Driving cycle	Represented driving condition	Distance km
LU-BS or BS	Urban short circuit loop free flow	5.8
Headingley	Urban free flow and slow/congested flow	4.4
HR-part1	Urban free flow and slow/congested flow	4.0
HPL-A	Urban large circuit loop, left turns at junctions	4.5
HPL-B	Urban large circuit loop, right turns at junctions	4.5

The ambient temperatures when these five tests were carried out were 11~20 °C. So there is little influence of ambient temperatures on engine warm up and emissions.

RESULTS

SPEED PROFILE

The vehicle travel speed was logged at 1Hz and plotted against time shown in figure 6 for all five journeys. The BS journey represented a free flow urban driving pattern with regular stops at traffic lights. The four loops had a good repeatability. The Headingley journey represented a mild congestion journey which started with normal free flow driving and stops and then experienced a short traffic queue from 300 to 430 seconds. The HR-part1 journey was a typical congested traffic scenario. The vehicle had an initial short period of cruising at around 150 second and then started stop-start congested driving period from 220 to 720 seconds. The HPL-A and HPL-B were driven on the same route but different direction: anticlockwise and clockwise. The different travel direction made a remarkable difference in speed profile of two journeys as the left or right turning at each junction was a significant factor that affects the driving and therefore emissions. The speed profile of HPL-A in figure 6 showed that the journey had typical stops at junctions controlled by traffic lights and cruising between stops. The HPL-B journey showed there were some stops at junctions similar to the HPL-A but some significantly long stops appeared due to the right turn which had to give way to the oncoming traffic.

Figure 7 shows the accumulated traveled distance and speed profile for five journeys. The BS journey had the longest distance of 5.8 km. The HR-part1 journey had shortest distance of just over 4 km.

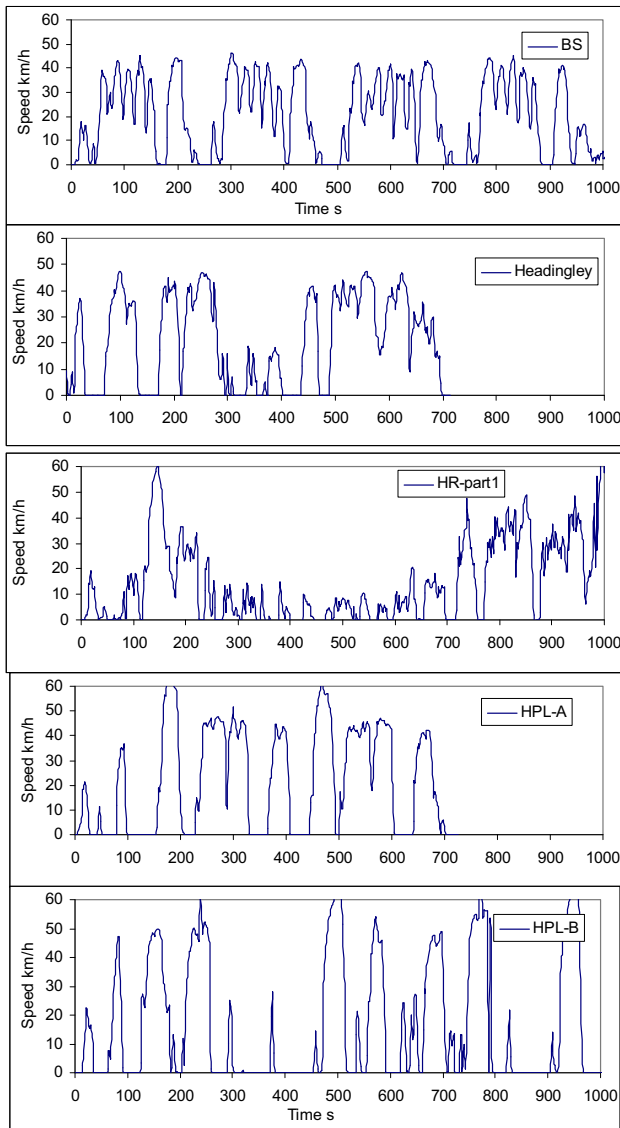


Figure 6: Road speed profile of five journeys

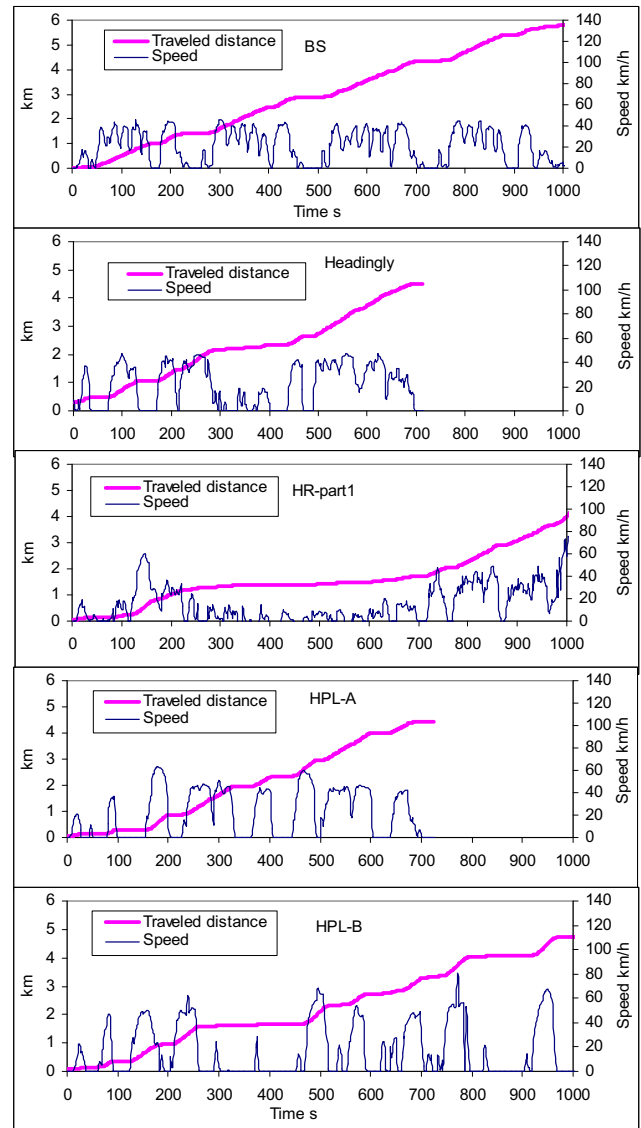


Figure 7: Traveled distance and speed as a function of time for five journeys

WARM-UP OF THE ENGINE COOLANT, LUBRICANT AND TWC

The engine out cold start emissions are influenced by the thermal inertia of the engine and engine cold start strategies such as spark timing, fuel injection system and air/fuel ratio enrichment. For a given engine, influence of cold start on engine out emissions is mainly due to the thermal inertia of the engine, coolant water and lubricating oil systems. The cold start influence on the catalyst performance is mainly due to the thermal inertia of the exhaust manifold, the downpipe and the underfloor catalyst.

Warm-up of the engine coolant water and lubricant

Figure 8 shows the warm up of engine coolant water and lubricating oil as a function of engine warm up for five journeys.

The full warm up of the coolant water is determined by the time the coolant water temperature reached the

fully warmed up value, when the thermostatic control valve opened and water temperature curve fell or was flat due to that the cold water in the radiator was added to the cooling water circulation. The full warm up of lubricating oil is defined here as the lubricating oil temperature reached the full warmed-up value (80°C). The results in figure 7 show that the BS, Headingley and HPL-A journeys had shorter water warm up period (about 340 seconds) that other two driving journeys. The water warm up period for HR-part1 journey was about 420 seconds and this period was increased to 500 seconds for HPL-B journey.

The warm up of the lubricating oil was much slower than the coolant water. The time needed for the lubricating oil to reach full warm up temperatures (80°C) was 600 seconds for BS journey, 660 seconds for Headingley journey, 820 seconds for HR-part1 journey, 660 seconds for HPL-A cycle and 780 seconds for HPL-B journey.

The warm up period of the lubricating oil was taken as when the lubricating oil reached 80°C. Two lubricating oil temperatures were measured (T10 and T18), one close to the surface of the lubricating oil (dipstick, T10) and one close to the bottom of the sump (T18). The top temperature is higher than the bottom as the oil from its circuit around the engine is heated and hence accumulates on the top of the sump oil level. The oil pump picks up cold oil from the bottom of the sump. Hence the true lube oil warm-up temperature is that for the bottom of the sump.

These results demonstrated that for the urban driving the coolant water needed at least about five and a half minutes to be fully warmed up. The lubricating oil needed at least 10 minutes to be fully warmed up. This period becomes longer if the traffic is congested. For the short urban journeys that are common in cities such as Leeds with a high population density (1,300/km²) these results show that the slow warm-up of the coolant water and lubricating oil are significant factors in the higher engine out emissions and fuel consumption under cold start, which are detailed below. Normally, the lube oil is unlikely to warm up in any short urban journey and this has a major impact on the higher fuel consumption in urban driving.

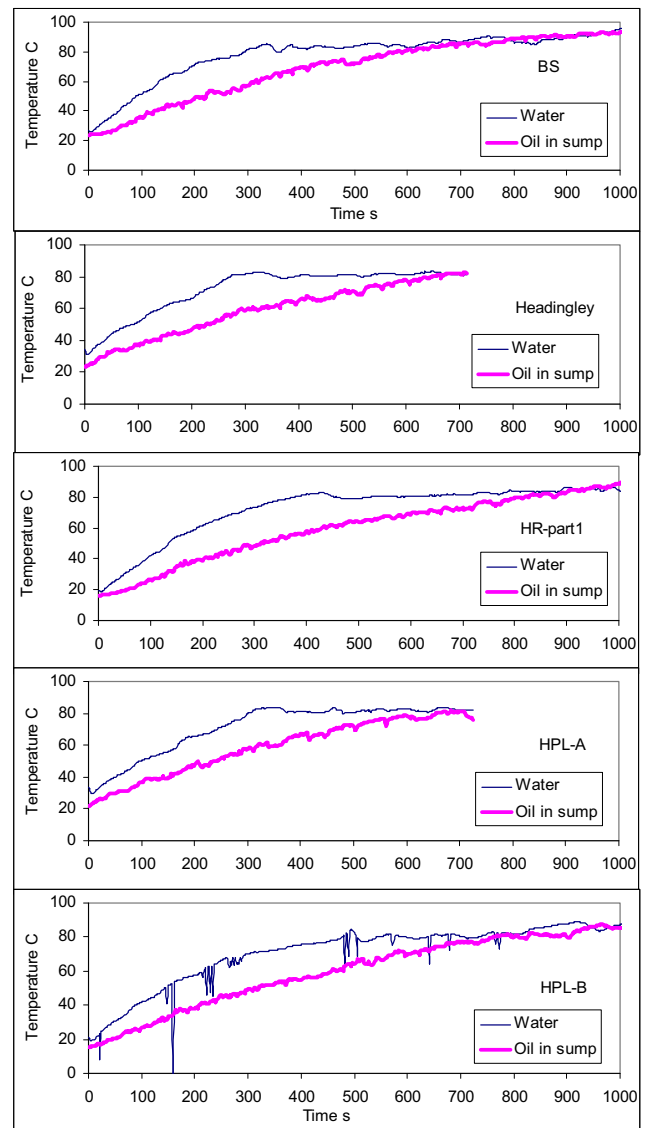


Figure 8: Warm up of coolant water and lubricating oil for five driving cycles

WARM UP OF THE CATALYST

Figure 9 shows upstream, middle and downstream of the TWC exhaust gas temperatures for five journeys. The catalyst inlet gas temperatures (upstream of the TWC) were dominated by the vehicle speed which was in fact directly affected by the exhaust gas volume. The middle gas temperature is a good indicator for the TWC light off, for which the authors had studied and reported before [3-4]. When the middle gas temperature reached 300°C and above the upstream of the TWC gas temperature the TWC was lit off. The downstream of the TWC gas temperatures reflected the TWC catalytic conversion efficiency. When this temperature reached typical catalyst light off temperature 300°C it was regarded as the TWC was in fully function.

The light off time of the TWC was 100 seconds for BS, 150 seconds for Headingley and HR-part1, 190 seconds for HPL-A and HPL-B. The time when the downstream of the TWC gas temperatures reached 300°C was 120 seconds for BS, 220 seconds for

Headingly and HPL-A, 190 seconds for HR-part1 and 210 seconds for HPL-B.

The figure 9 showed that the BS journey had highest TWC gas temperatures throughout the journey. However, the middle and downstream of the TWC gas temperatures after cold start were always above 300°C for all five journeys. The journey HR-part1 had about 500 seconds very low speed driving in a traffic queue and the mid and downstream of the TWC gas temperatures were still at around 400°C. The journey HPL-B had about 200 seconds idling from 250 to 450 seconds and the mid and downstream of the TWC gas temperatures were at around 350 and 400°C. The high mid and downstream of the TWC gas temperatures indicated the effective catalytic conversion operation, which give an effective control on the emissions.

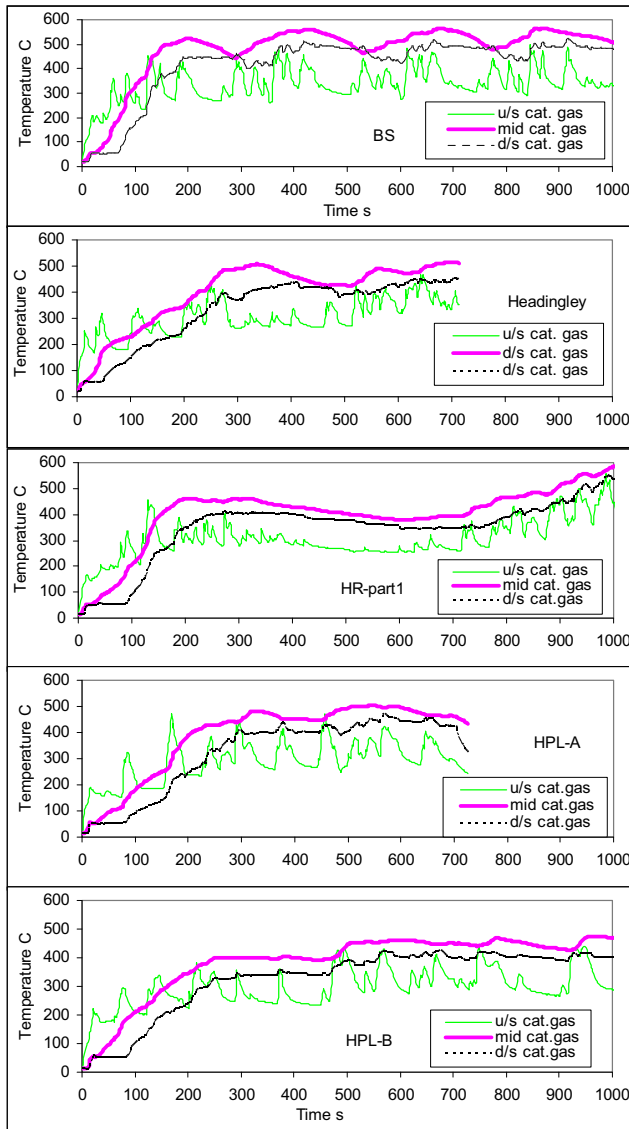


Figure 9: Warm up of the TWC for five driving cycles

LAMBDA VARIATION DURING COLD START AND FUEL CONSUMPTION

Figure 10 showed the lambda variation as a function of time for five journeys. The initial cold start rich period

(lambda < 1.0) was in a range of 40~70 seconds. The BS journey had more variations of lambda values than others. This was because the BS journey had more accelerations and decelerations and less idling period. The HPL-B journey had least lambda fluctuations as it had more idling period. The fluctuation of lambda reflected the engine operation mode. The lean spikes actually indicated that the catalytic converter was in open loop operation which occurred during deceleration process. The open loop operation may incur increased emissions. The fraction of open loop operation can be used to indicate the severity of real world driving cycles.

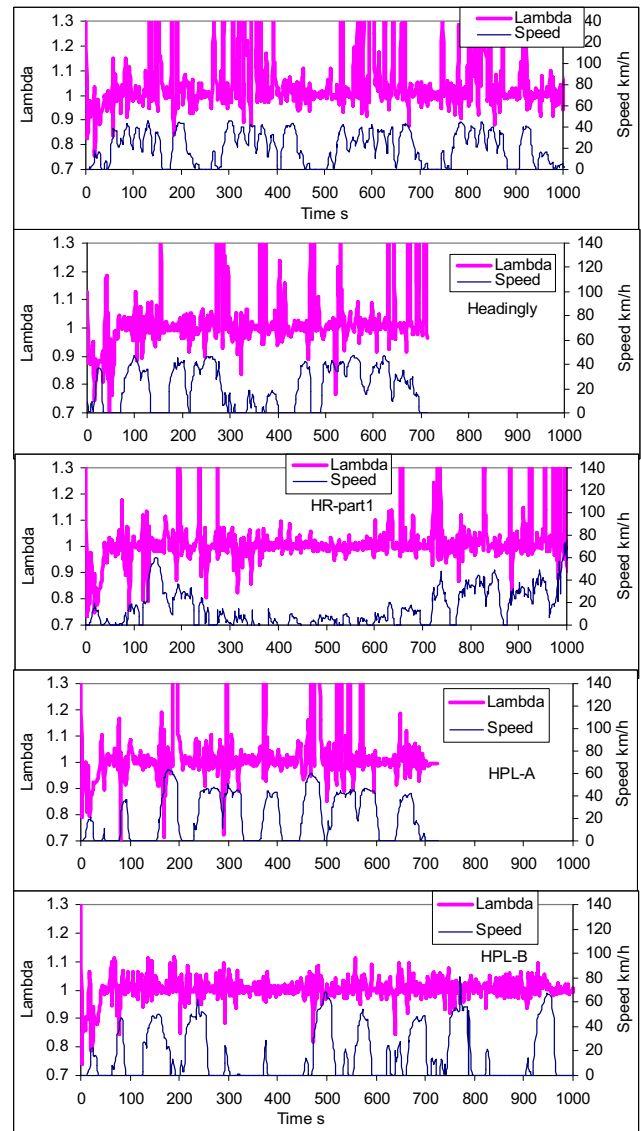


Figure 10: Lambda variations for five driving cycles

Fuel consumption for all five journeys is shown in figure 11. The results showed that the fuel consumption is directly responded to variation of vehicle driving speed.

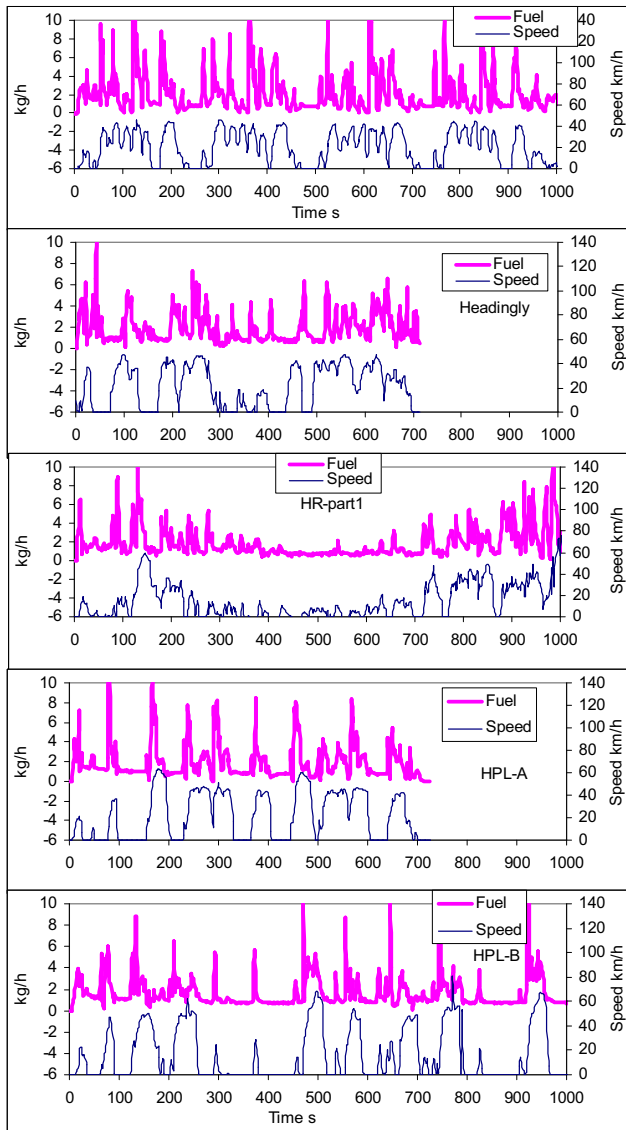


Figure 11: Fuel consumption for five driving cycles

GREENHOUSE GAS (GHG) EMISSIONS

Exhaust emissions were measured downstream of the TWC. Both the regulated emissions and non-regulated emissions were monitored as a function of engine warm up for the five journeys. The greenhouse gases: CH₄, CO₂ and N₂O were analyzed for mass emission rate g/s and accumulative mass g as shown in figures 12, 13 and 14.

Methane emissions

The methane emissions in figure 12 showed a different profile for different journeys. The BS journey had an apparent chunk peak of transient mass emissions during the first 150 seconds. For the Headingly journey, the apparent cold start peak lasted for 50 seconds where a significant change of gradient of accumulated mass occurred. However, the methane mass emissions were still high till about 300 seconds. The high cold start peaks of methane emissions were not shown clearly for other three journeys. After the

initial high emissions period, the methane mass emissions were at significantly lower magnitude but still notable for all journeys. The gradient of accumulated methane mass curve was smaller and yet continued to increase for BS, Headingly and HR-part1 journeys. For HPL-A and HPL-B journeys, there were no clear cold start chunks for methane emissions though the methane emissions were higher in the first 50 seconds. For all journeys, the methane emission peaks were visible and the accumulated methane mass was increasing steadily throughout the whole journey. Combined with the TWC mid and downstream gas temperatures in figure 9, a light off time of the TWC for methane conversion from cold start can be determined, which was defined as the end of the initial high methane emission peaks plus the downstream of the catalyst gas temperature reached 300~350°C. For different journeys, this light off time and therefore distance were different as shown in table 3. The BS journey had shortest light off time and distance due to short idling after the engine start and quick picking up of the speed.

Table 3: TWC light off time for methane emissions

	Light off time seconds	Light off distance km
BS	150	0.94
Headingly	250	1.79
HR-part1	200	1.01
HPL-A	250	1.05
HPL-B	250	1.47

The accumulated methane mass emissions were converted into distance based emission in unit of g/km. Figure 13 showed the distance based methane emissions for all five journeys. The emissions here were expressed using three terms: Whole Journey mean (WJ), cold (mean emissions for the period before the TWC light off) and hot (mean emissions for the period after TWC light off to the end of tests). The results in figure 13 showed that HR-part1 had the highest whole journey mean methane emissions (0.075g/km) and other four journeys produced similar level of journey mean methane emissions (~0.05g/km). For cold stage mean methane emissions, HR-part1 was the highest followed by BS and HPL-A. The journey HPL-B produced lowest methane emissions before the TWC was lit off. The variation of distance based methane emissions before the light off of the TWC between different journeys was significant. After the TWC was lit off, the hot stage methane emissions were reduced significantly. The free flow driving journey BS and Headingly produced lower methane emissions in terms of g/km than that of the congested journey HR-part1 and long idling journeys HPL-A and HPL-B.

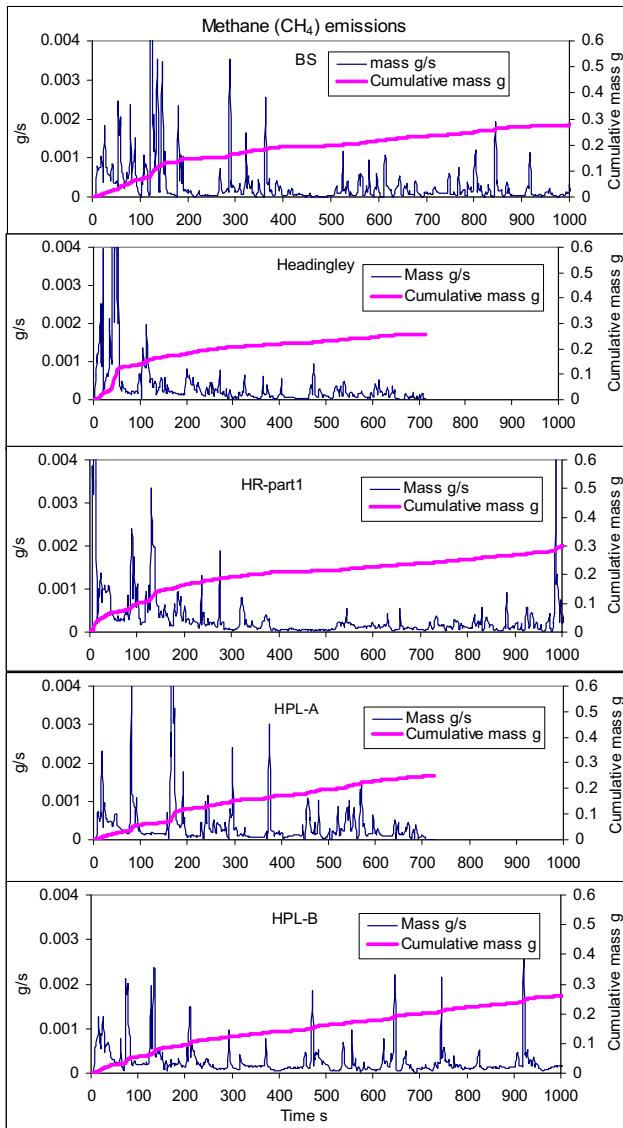


Figure 12: Methane (CH₄) emissions as a function of engine warm up for five driving cycles

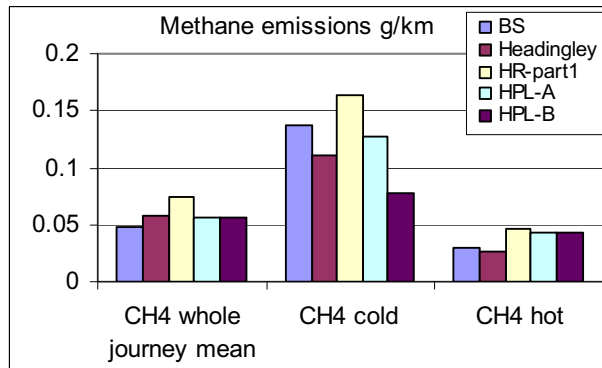


Figure 13: Distance based methane emissions for whole journey, cold and hot sections

Figure 14 compared the cold to hot stage methane emissions as well as comparison with whole journey mean methane emissions in terms of g/km. The cold stage methane emissions by g/km were at least 30% higher than whole journey mean emissions and could be 1.9 times higher. The hot stage methane emissions by g/km were about a half to three quarters of whole

journey mean emissions. The methane emissions before the TWC lit off was 0.9~3.5 higher than that after the TWC lit off.

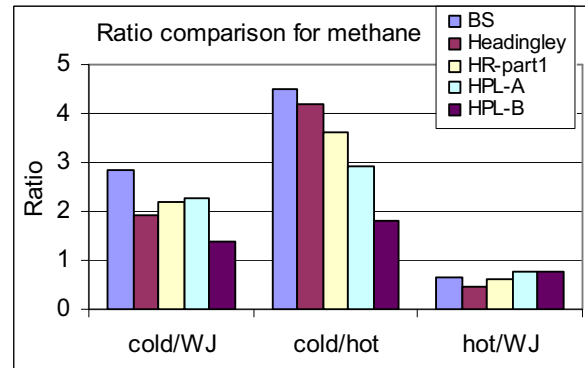


Figure 14: Comparison between whole journey (WJ), cold start and hot stage methane emissions for all five journeys

CO₂ emissions

The CO₂ emissions are a dominant greenhouse gas emitted in that the mass of CO₂ emissions are much higher than other two greenhouse gases. The CO₂ emissions in figure 15 were a direct reflection of driving speed and thus fuel usage. The CO₂ mass emission rate during idling was about 1 g/s. The peak value can be up to 5~6 g/s. The idling CO₂ mass emission rate was low but when considering the distance based mass emissions in the congested traffic scenario, long period idling will have a significant contribution to distance based mass emissions.

Figure 15 did not show an apparent cold start peaks for CO₂ emissions. The identified cold start stage (before the TWC light off) for methane emissions in table 3 was used to investigate the cold start stage and hot stage distance based CO₂ emissions. Figure 16 shows the distance based CO₂ emissions for the whole journey mean, cold stage and hot stage mean CO₂ emissions for all five journeys.

The whole journey mean CO₂ emissions by g/km varied from 230 to 390 g/km between five different journeys. The cold and hot stage CO₂ emissions were similar. Figure 17 shows the comparison between hot and cold as well as with whole journey mean CO₂ emissions. Only journey HPL-A showed the cold start effect on CO₂ emissions and all other journeys showed no difference between hot and cold CO₂ emissions.

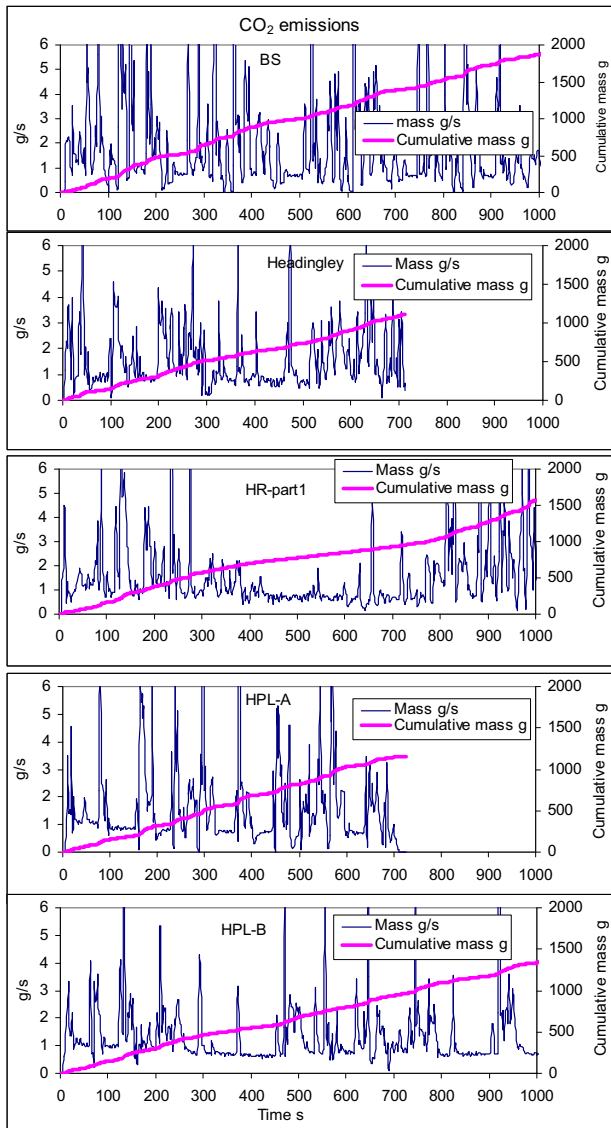


Figure 15: CO₂ emissions as a function of engine warm up for five driving cycles

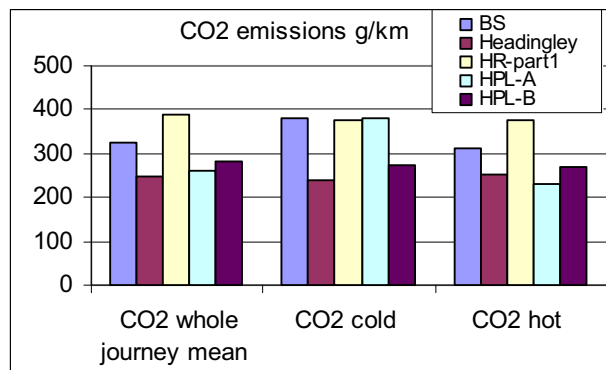


Figure 16: Distance based CO₂ emissions for whole journey, cold and hot sections

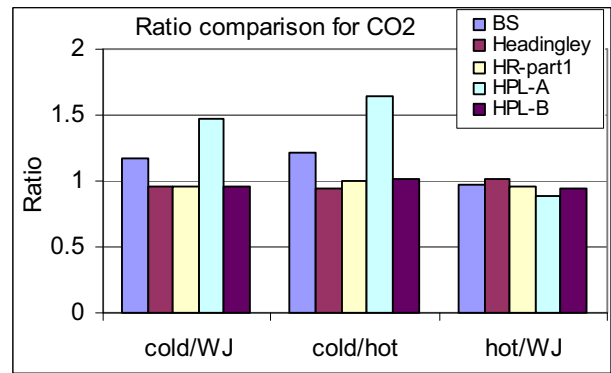


Figure 17: Comparison between whole journey (WJ), cold start and hot stage CO₂ emissions for all five journeys

Nitrous oxide emissions

Nitrous oxides are formed over TWC during the warm up period of the TWC when the temperature of TWC was around 250 – 350°C, thus an association of N₂O with the end of the catalyst warm-up period is expected. N₂O can also be formed during any transient if the temperature falls into this region. The nitrous oxide emissions for five journeys are shown in figure 18.

For BS journey, there were two large peaks of nitrous oxide emissions from 50 to 150 seconds, the end of the TWC light off period. There was then intermittent N₂O generation throughout the rest of the journey. The accumulated N₂O mass had been increased consistently throughout the whole journey. For Headingley journey, two large peaks appeared at 100~150 seconds and 200 ~300 seconds which were associated with the mid and end of TWC warm up period. The journeys HR-part1, HPL-A and HPL-B did not show apparent nitrous oxide peaks during the TWC warm up process, but there were remarkable peaks in the rest of the journeys. For HR-part1 journey, the 500 seconds of low speed crawling driving in the congested traffic hardly produced any nitrous oxide emissions due to perfect lambda one control. However, the low speed driving could not maintain the TWC temperature high enough and therefore once the vehicle re-entered the free flow driving, a series of nitrous oxide emission peaks appeared. For journey HPL-B, the long idling of the engine at the junctions made the TWC temperatures low, thus when the vehicle suddenly accelerate to leave the junction a high nitrous oxide emission peak was produced.

Unlike the methane emissions, the nitrous oxide emissions did not show a clear cold start peak for any one of the five journeys. Only the free flow journey BS and Headingley had a couple of relatively large peaks during warm up process.

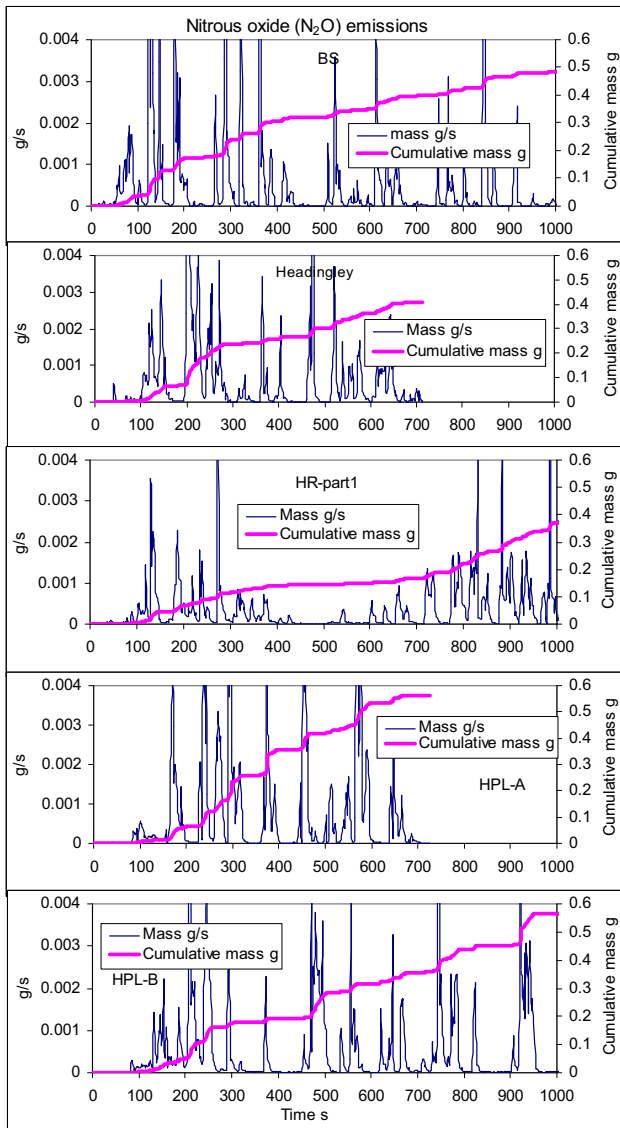


Figure 18: Nitrous oxide (N₂O) emissions as a function of engine warm up for five driving cycles

GLOBAL WARMING POTENTIAL (GWP)

In 1990s, IPCC (the Intergovernmental Panel on Climate Change) proposed and developed the concept: Global Warming Potential (GWP) after an extensive work being carried out. The Global Warming Potential (GWP) is a concept to provide a simple measure of the relative radiative forcing of the different greenhouse gas emissions and estimate possible warming effect (relative) on the atmosphere by greenhouse gas emissions. The GWP is defined as the cumulative radiative forcing between the present and a chosen future time scale caused by a unit mass of gas emitted now, expressed relative to that for some reference gas (CO₂ is normally used). The GWP of a particular GHG over a chosen time scenario is calculated by the GWP of that GHG multiplied by the amount of the gas emitted. Table 4 presented the relative GWP index for CO₂, CH₄ and N₂O normalized to CO₂ and published by IPCC in 1995 [11]. The life time for CO₂ varied a lot depending on sources and passages of decay. The methane has a relative short

lifetime in the atmosphere mainly due to the reaction with troposphere hydroxyl radical and uptake by soils. The nitrous oxide has a long atmospheric life time (~120 years) and large radiative forcing.

Table 4: Relative GWP of greenhouse gases

Species	Lifetime Years	GWP	
		20 years	100 years
CO ₂	50~200	1	1
Methane CH ₄	12±3	56	21
Nitrous oxide N ₂ O	120	280	310

The contributions of CO₂, methane and nitrous oxide to GWP were calculated using GWP index in table 4. Then the fractions of each gas GWP for each journey were determined and presented in figure 19 for 20 years scenario and figure 20 for 100 years scenario. For both time scenarios, the contributions of three GHGs to GWP for all five journeys were approximately 90±3 % for CO₂, 10±3 % for N₂O and 0.3~1.2% for methane.

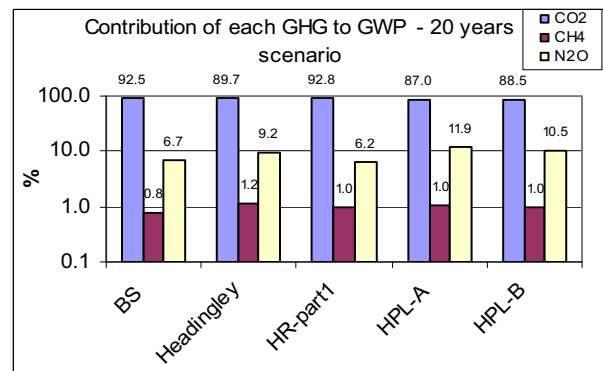


Figure 19: Contribution of each GHG to GWP in terms of whole journeys for all five journeys based on 20 years scenario

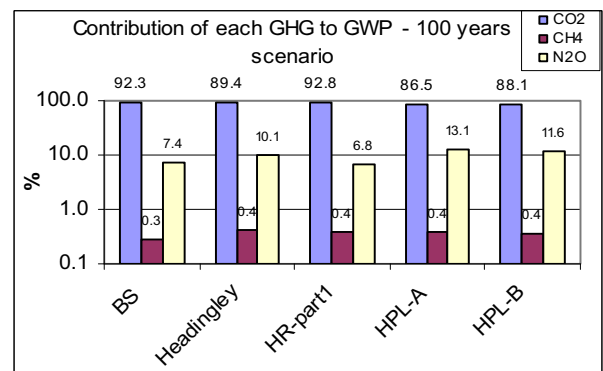


Figure 20: Contribution of each GHG to GWP in terms of whole journeys for all five journeys based on 100 years scenario

CONCLUSION

Five real world driving cycles were designed to represent five different urban driving conditions including free flow driving, congested slow moving driving and long idle driving at junctions. One typical journey for each driving cycle was analysed and reported in this paper. A EURO 2 emission compliant SI passenger car was used. The engine warm up including coolant water, lubricating oil, and the TWC temperatures were monitored. Real time fuel consumption and lambda were measured. The exhaust emissions were measured using an on-board FTIR real time emissions measurement system. Three GHG CO₂, N₂O and CH₄ emissions were measured. The results show:

1. The time needed to fully warm up engine coolant water was 340 to 500 seconds and to fully warm up engine lubricating oil was 600 to 780 seconds depending on driving cycles. The cycle HPL-B with long idling at junctions had slowest warm up for coolant water and lubricating oil.
2. The TWC light off time for methane conversion was 150 to 250 seconds for all five journeys. The free flow driving BS has fastest TWC light off.
3. The initial fuel rich period ($\lambda < 1$) for cold start was 40~70 seconds for five journeys. The free flow driving BS with small driving circuit had more lambda fluctuations due to more turning events.
4. The methane emissions had a clear cold start stage indicated by high emission peaks. All five cold start journeys had similar levels of cold start methane peaks and accumulated mass. The methane emissions by g/km before the TWC light off were approximately 2~4 times as high as that after the TWC light off.
5. The CO₂ emissions did not have a clear cold start peak. The CO₂ mass emissions were varied between 1 g/s at idle and 5~6 g/s at 50~60 km/h.
6. The nitrous oxide emissions peaks occurred for some journeys from the mid to the end of the TWC warm up periods. The congested traffic hardly produced any nitrous oxide and yet when the vehicle left the congested traffic and picked up speed, nitrous oxide peaks were produced. Also when the vehicle left a junction after a long waiting, the vehicle produced significant nitrous oxide emissions.
7. The assessment of GWPs by three GHGs showed that the CO₂ emissions contributed approximately 90±3% and the nitrous oxide had about 10±3% contribution whereas the methane emissions only had less than 1% contributions.

ACKNOWLEDGMENTS

We would like to thank the UK EPSRC for a research grant, GR/M88167/01, for a JIF (Joint Infrastructure

Fund) award for the LANTERN project (Leeds health Air quality, Noise, Traffic, Emissions Research Network). We would also like to thank the EPSRC for the research grant, GR/S31136/01, for the RETEMM (Real-world Traffic Emissions Measurement and Modeling) project award in support of this work. Thanks also go to Bob Boreham for his technical support and expertise. Basil Daham would like to thank the University of Leeds for a research scholarship.

REFERENCES

1. Hans P and Cozzarini C, *Emissions and air quality*/ SAE Reference book R237. 2000: SAE International.
2. *UK national atmospheric emissions inventory website: <http://www.naei.org.uk>*. [cited].
3. Andrews GE, Zhu G, Li H, Simpson A, Wylie JA and Bell M. and Tate EJ, *The Effect of Ambient Temperature on Cold Start Urban Traffic emissions for a Real World SI Car*. SAE Technical Paper Series 2004-01-2903. 2004: SAE International
4. Andrews GE, Li H, Wylie JA, Zhu G, Bell MC and Tate EJ, *Influence of Ambient temperature on Cold-start Emissions for a Euro 1 SI Car using in-vehicle Emissions measurement in an Urban Traffic Jam Test Cycle*. SAE Technical Paper Series 2005-01-1617. 2005, SAE International.
5. Li H, Andrews GE, Daham B, Bell MC, Tate JE and Ropkins K, *Impact of Traffic Conditions and Road Geometry on Real world Urban Emissions Using a SI Car*. SAE Technical Paper Series 2007-01-0308, in *Emissions measurement and testing, 2007 (SP-2089)*. 2007, SAE International.
6. Li H, Andrews GE, Khan AA, Savvidis D, Daham B, Bell MC, et al., *Analysis of Driving Parameters and Emissions for Real World Urban Driving Cycles using an on-board Measurement Method for a EURO 2 SI car*. SAE Technical Paper Series 2007-01-2066/JSAE 20077353, in *The JSAE International Fuels and Lubes Conference 2007*, SAE International/JSAE: Kyoto, Japan.
7. Li H, Andrews GE, Savvidis D, Daham B, Ropkins K, Bell MC, et al., *Study of thermal characteristics, fuel consumption and emissions during cold start using an on-board measuring method for SI car real world urban driving*. SAE Technical Paper Series 2007-01-2065, in *The JSAE International Fuels and Lubes Conference 2007*, SAE International/JSAE: Kyoto, Japan.
8. Li H, Andrews GE, Savvidis D, Daham B, Ropkins K, Bell MC, et al., *Comparisons of the exhaust emissions for different generations of SI cars under real world urban driving conditions*. SAE Technical Paper Series 2008-01-0754, in SP2150. 2007, SAE International.
9. Li H, Ropkins K, Andrews GE, Daham B, Bell MC, Tate JE, et al., *Evaluation of a FTIR Emission Measurement System for Legislated Emissions Using a SI Car*. SAE Technical Paper Series 2006-01-3368, in *Proceedings of Powertrain & Fluid Systems Conference*. 2006, SAE International: Toronto, Canada.

10. Department of the Environment and T.a.t. Regions, *The Environmental Impacts of Road Vehicles in Use*. 1999.
11. Houghton, J.T., et al., *Climate Change 1995 - The Science of Climate Change*, ed. J.A. Lakeman. 1995, Cambridge: The Intergovernmental Panel on Climate Change, Cambridge University Press.

CONTACT

All contact please direct to Dr. H Li, Energy and Resources Research Institute, The University of Leeds, Leeds. LS2 9JT, UK. Email: fuehli@leeds.ac.uk

ABBREVIATIONS

CO: Carbon monoxide.
CO₂: Carbon dioxide.
CVS: Constant Volume Sampling.
ECE: Economic Commission for Europe.
FTIR: Fourier Transform Inferred.
GHG: Greenhouse gas.
GWP: Global Warming Potential.
LU-BS: Leeds University Business School driving cycle.
LU-UDTC: Leeds University Urban Driving Test Cycle.
LU-HR: Leeds University Headingley Ring road cycle.
LU-HPL: Leeds University Hyde Park Loop cycle.
NEDC: New European Driving Cycle.
NO_x: Nitrogen Oxides.
N₂O: Nitrous oxide.
SI: Spark Ignition.
TWC: Three Way Catalyst.